Structural Investigation of the Dopamine-2 Receptor (D2R) Agonist Bromocriptine Binding to Dimeric $D2^{High}R$ and $D2^{Low}R$ States

Ramin Ekhteiari Salmas[1]*, Philip Seeman[2], Matthias Stein[3], Serdar Durdagi[1,4]*

[1]Computational Biology and Molecular Simulations Laboratory, Department of Biophysics, School of Medicine, Bahcesehir University, Istanbul 34349, Turkey
[2]Departments of Pharmacology and Psychiatry, University of Toronto, 260 Heath Street West, Unit 605, M5P 3L6, Toronto, Ontario, Canada
[3]MaxPlanck Institute for Dynamics of Complex Technical Systems, Molecular Simulations and Design Group, Sandtorstrasse 1, 39106, Magdeburg, Germany
[4]Neuroscience Program, Graduate School of Health Sciences, Bahcesehir University, Istanbul 34349, Turkey

***Corresponding Authors:**

Ramin Ekhteiari Salmas, Ph.D. (ekhteiarisalmas@itu.edu.tr)

Serdar Durdagi, Ph.D. (serdar.durdagi@med.bau.edu.tr)

ABSTRACT: The active ($D2^{High}R$) and inactive ($D2^{Low}R$) states of dimeric dopamine D2 receptor (D2R) models were investigated to clarify the binding mechanisms of the dopamine agonist bromocriptine, using Molecular Dynamics (MD) simulation. The aim of this comprehensive study was to investigate the critical effects of bromocriptine binding on each distinct receptor conformation. The different binding modes of the bromocriptine ligand in the active and inactive states have a significant effect on the conformational changes of the receptor. Based on the MM/GBSA approach, the calculated binding enthalpies of bromocriptine demonstrated selectivity toward the $D2^{High}R$ active state. There was observed agreement between the calculated and experimentally measured $D2^{High}R$ selectivity. In the ligand-binding site, the key amino acids identified for the $D2^{High}R$ were Asp114(3.32) and Glu95(2.65), and for the $D2^{Low}R$ it was Ser193(5.42). Moreover, replicate MD trajectory analyses demonstrated that the bromocriptine binding site conformational structure was more rigid for the $D2^{High}R$ state and a more flexible for the $D2^{Low}R$ state. However, the side chains of the ligand-receptor complex of the $D2^{High}R$ showed larger variations relative to the corresponding regions of the $D2^{Low}R$. The present study is part of an ongoing research program to study D2R conformational changes during ligand activation and to evaluate the conformational state selectivity for ligand binding.

INTRODUCTION

G protein-coupled receptors (GPCRs) constitute the largest family of cell-surface receptors that are involved in cell signal transduction pathways that regulate numerous cellular processes in human tissues. The GPCRs are considered as one of the most important group of drug targets in medicine [1,2]. Since GPCRs are targeted by nearly 40% of marketed drugs, a better understanding of the respective ligand binding mechanisms and signal transduction processes will aid the identification of novel therapeutics that specifically target GPCRs [3-5]. Although GPCRs share a common feature of a 7 transmembrane (TM) spanning domain, these transmembrane helices still present many challenges in terms of crystal structuring, as they are embedded within the lipid bilayer [6]. To date, the number of determined crystal structures is approximately 30 for class A GPCRs. While most structures are resolved in the inactive state of the receptor and typically bound to an antagonist or inverse agonist, there are several receptor structures that have been resolved in the agonist-bound active state. Molecular modeling approaches play an integral role in predicting 3D structures of GPCRs, by utilizing known GPCR templates [7-11]. Our understanding of GPCR structures, utilizing either crystallographic data or homology models, can thus provide significant information and guide the ligand design process [11].

The homology modeling approach for unresolved crystallographic structures plays an integral role in GPCR-based studies by addressing physiological and pharmacological functions of the ligand-binding domain, G protein-coupled activity, and signal transduction. This approach primarily leads to the design of more effective drugs, acting by either inhibition or activation of GPCR activity [11]. Most importantly, these cost-efficient and rapid-process modeling approaches can be extended and applied to many GPCRs [12-14].

The current study focuses on the dopamine D2 receptor (D2R) and its structural role as a drug target to treat Parkinson's disease (PD), various psychotic disorders [15-17], and particularly the common prolactinomas of the anterior pituitary gland. The D2R is recognized as a therapeutic target for antipsychotic and antiparkinsonian agents, by antagonizing and stimulating dopamine-dependent

receptors, respectively [15-17]. Although the exact function and activation of the D2R in controlling the signal transduction pathways of the central nervous systems are not well known, the D2R is believed to be also a prime therapeutic target for mental and neurodegenerative disorders, including schizophrenia [18-21].

It is known that the D2R, as well as most other GPCRs, exhibit functionality mainly as homo- or hetero- dimers and as oligomers [22-24]. However, there is a broad spectrum of computational studies that evaluate monomeric GPCRs to investigate ligand-binding as well as the triggered conformational changes of the entire system upon binding [9,25]. In the monomer-based studies, a significant link between the efficacy and specificity of the ligand and either homo-/hetero-dimerization or oligomerization has not been considered to date. Since the first GPCR dimerization studies appeared, GPCR (including the D2R) homodimerization and heterodimerization were studied extensively by experimental and computational research groups to elucidate possible GPCR pairing [26]. The majority of the D2R dimerization/oligomerization studies focus on how the protomers interact with each other and which TM segments play a crucial role in protein-protein interfacing. Data from several studies demonstrated that protomers dimerize via the TM4 interface [27-29]. Among the crystallographic structures of the GPCR, a small number of dimer formations have been reported. For example, crystal structures of squid rhodopsin (PDB ID: 2Z73) and oligomeric beta-1-adrenergic (PDB ID: 4GPO) receptors are available and suggest dimerization of the receptors and a role of the TM4 domain in the dimeric interface. Rhodopsin is one of the most highly studied receptors of the GPCR family and its native oligomeric arrangement has been depicted by Fotiadis et al [30], using atomic force microscopy (AFM) and semi-empirical dimer models of TM4/TM5 interfaces that were constructed and simulated using classical MD techniques. This study also led to another study that evaluated cross-linking of substituted cysteine residues within the TM4 and TM5 domains of the D2Rs [27].

Petersen et al., in a groundbreaking investigation of dimer dissociation and formation of GPCRs, studied the Frizzled 6 (FZD 6) receptor (Class F GPCR), using both mutational analysis and

modeling approaches [31]. This study suggested that the TM4 and TM5 domains primarily contributed to dimer interfacing of the FZD 6 GPCR [31].

Previous studies suggested the co-existence of dimeric and monomeric forms of the D2R as well as cross-linking upon homodimerization from TM4 and TM5. These data were consistent with results from Guo et al [27,32] and Petersen et al [31].

Furthermore, it should be noted that other GPCR TM domains may be involved in dimer formation [29]. In a study that evaluated the self-assembly behavior of rhodopsin, in which up to 64 molecules of the GPCR were inserted into a model membrane and simulated for μs length using coarse-grained MD (CGMD) method, the TM1/helix-8 and the TM4/TM5 interfaces were both found to be relevant for the self-assembly process [33].

The fully activated and inactivated states, as well as the dimeric forms, of the D2R can be differentially stabilized upon various interactions with small molecules within the binding cavities. Hence, such selectively targeted interactions may be a means to manipulate relevant signaling pathways for potential treatment options [27,28]. The existing experimental evidence describing binding affinities of the D2R ligands in the active sites of the $D2^{High}R$ and $D2^{Low}R$ suggests that dopaminergic stabilizers selectively interact with the $D2^{High}R$ conformation with a higher binding affinity, as compared to the $D2^{Low}R$ state [10,34].

In the present study, the fully activated and inactivated D2R dimer models were utilized as potential targets of the bromocriptine agonist to investigate the structural and dynamic effects upon ligand binding [34-36]. Specifically, this study investigates the binding mechanism of bromocriptine, which is a well-known treatment option for Parkinson's disease (PD) as well as for common pituitary prolactinomas. Bromocriptine has an elongated (not bulky) structure that allows for a more adequate fit within the active site binding pockets of the D2Rs. Our previous study on D2R ligands [10], which focused on the smaller-sized more rigid molecules (eg, apomorphine and dopamine), identified the binding mechanisms for both the monomeric and dimeric states of the D2R. However, due to limited conformational space within the binding pockets of these molecules for the agonist,

the behavior of elongated and larger structural agonists such as bromocriptine may be more complex as they are able to bind more amino acids with more variable interactions relative to smaller ligands. Furthermore, in the current work, both backbone and side chains atoms that were involved in the conformational changes were thoroughly investigated by considering the individual effects of the side chain and backbone atoms based on their RMSD and RMSF profiles. By separating out the effects of backbone and side chain atoms from those elicited by the conformational changes, a further clarification of agonist binding to the $D2^{High}R$ and $D2^{Low}R$ from a structural and dynamic standpoint was achieved. In addition, the movements of the protein for both D2R conformations upon agonist binding were simulated.

More specifically, the current study focuses on the following points: (i) how an agonist with an elongated structure acts when it binds to the distinctly stabilized forms of the D2R; (ii) evaluation of the dynamics and conformational behavior of the agonist in the active sites throughout the MD simulations; (iii) assessment of how the ligand-binding domains of the active and inactive D2R states lead to the conformational changes occurring in the cytoplasmic ends of the TM5 and TM6 domains; and (iv) determination of the key amino acids involved in ligand binding and their role within the binding domain to stabilize bromocriptine; (v) individual contributions of the backbone and side chains atoms in terms of conformational change when the ligand binds to the $D2^{High}R$ and $D2^{Low}R$ sites.

In earlier studies, the monomeric and dimeric models of the active and inactive D2R states were used to evaluate the binding mechanisms of antipsychotic drugs in different conformational environments of the D2R [10]. It was suggested that receptor dimerization shows negative cooperativity on the ligand-binding domain [10,29]. In addition, these studies highlight which amino acids (within the ligand-binding sites) are involved in receptor inhibition or stimulation for both the active and inactive D2R conformations. The present study used homology modeling structures of the D2R in both the active ($D2^{High}R$) and inactive ($D2^{Low}R$) homodimeric forms from previously reported studies [9,22]. The main structural differences between the active and inactive

states of the D2R appeared on the cytoplasmic ends of the TM5 and TM6 domains. The most notable conformational changes include the outward movement of the TM6 cytoplasmic end to accommodate transducer binding the α-helical motion of the TM5 cytoplasmic end (see **Figure S1**). The present study is part of a continuing program to evaluate agonist-elicited conformational changes of the D2R and to assess potential effects, which may be direct or indirect, on the ligand-binding domain. Furthermore, this study clarified the potential involvement of backbone and side chains atoms in ligand-activated conformational changes. In terms of structural and dynamic properties, separating out the effects of the backbone and side chain atoms provides additional insight into agonist-activated protein movement for each D2R form.

MATERIALS AND METHODS

Ligand Setup

The initial structure of bromocriptine was retrieved from the Cambridge Crystallographic Data Centre (CCDC) and incorporated into the ligand preparation process using the LigPrep module [37]. The Epik code [38] was used to assign the molecule protonation state at a physiological pH (pH = 7.4) and an automatic conformer generator was implemented to search for the most stable structure. The Epik code, automatic conformer, and force field optimization were evaluated with the OPLS2005 module [39]. The electrostatic potential (ESP)-derived atomic charges for bromocriptine were calculated with the Austin Model 1 (AM1) semi-empirical method [40].

Homology Modeling

The dimeric D2R models of both $D2^{High}R$ and $D2^{Low}R$ were carefully constructed and validated in previous studies [10] and here used for subsequent simulations and investigations. Since the aim of this work is to investigate the effect of an agonist binding to the distinct active and inactive states of the D2R, the available crystal structures of β2-adrenergic receptor both in active and inactive states were used as templates in the homology modeling. This gives us a consistent choice of template structures. Since the D3R crystal structure (PDB: 3PBL [41]) was obtained only in inactive state with D3R antagonist eticlopride complex, it is not used as template structure in modeling. The β2-

adrenergic receptor provided an excellent basis for this work because it was the first mammalian G protein-linked receptor to be fully described on the structure of rhodopsin. Hence, the structures were generated based on X-ray templates of the fully activated and inactivated forms of the β2-adrenergic receptor, sharing an acceptable amino acid sequence homology with the D2R. The details of the modeling and dimerization processes have been described in our previous work [10]. The coordinate files of the $D2^{High}R$ and $D2^{Low}R$ dimer model structures are available as Supplementary Information.

System Setup and MD Simulations

The initial structures of the dimeric $D2^{High}R$ and $D2^{Low}R$ states were prepared using the Protein Preparation module of Maestro, involving molecular mechanics (MM) optimization and the protonation state assignment. Bond orders were assigned, hydrogen atoms were added, disulfide bonds were created. Protonation states at the physiological pH of 7.4 conditions were performed using PROPKA [42]. Bromocriptine was docked into the binding pockets of dimeric $D2^{High}R$ and $D2^{Low}R$, using the flexible Induced Fit Docking (IFD) approach [43]. Then, these receptor models were embedded into a dipalmitoylphosphatidylcholine (DPPC) membrane bilayer (128 lipids for both upper and lower leaflets) surrounding the protein-ligand complex. The systems were then solvated by explicit TIP3P water models [44] in a layer of 15 Å thickness on each side **(Figure S2)**. Neutralization was done by a Monte-Carlo ion placement method by adding 0.15 M NaCl**.** The MD simulations were carried out using Desmond software [45] in a periodic box with application of the particle-mesh Ewald method [46] to calculate the long electrostatic interactions. The energies of the atomic interactions were simulated, using the OPLS2005 force field with a cut-off radius of 10 Å. The Nose−Hoover thermostat [47] and Martyna−Tobias−Klein [48] methods were used to maintain the temperature (310 K) and pressure (1.01325 bar) of the system. The systems were minimized for a maximum of 5000 iterations until a convergence threshold of 1 kcal mol^{-1} $Å^{-1}$ was achieved. The systems were then relaxed, using a step-wise procedure and gradually equilibrated. Starting with different initial velocity distributions, six independent 100 ns MD simulations (in total 600 ns),

were performed without any constraints. Initiating simulations with a well-equilibrated D2R conformation system and utilizing the most likely conformation can aid in achieving optimal results from simultaneous simulations by providing enough flexibility to explore other conformational regions. Thus, one representative structure with the highest conformational similarity to the average structure from the first MD simulations was chosen and then incorporated into the second and third MD simulations as initial conformers with different seeding numbers.

Conformational Stability and Surface Area Assays

The conformational stability analyses and surface area calculations of the systems, including root-mean-square deviation (RMSD), root mean square fluctuation (RMSF), radius of gyration (rGyr), molecular surface area (MolSA), solvent accessible surface area (SASA), polar surface area (PSA) and dihedral angle analysis were carried out using tools from Desmond [45]. The default settings in the *Simulation Interactions Diagram* module in Desmond were used. While rGyr is a measure for the spatial extension of a ligand, MolSA gives the molecular surface with a 1.4 Å probe radius. SASA and PSA give the surface area of a molecule accessible by a water molecule and the solvent accessible surface area in a molecule from only oxygen and nitrogen atoms. All the graphs, involving line, contour and stacked bar plots, were generated with in-house Python scripts, using Matplotlib [49] and NumPy libraries [50]. The 2D and 3D schematic diagrams were prepared with Maestro and PyMOL visualizers. The pairwise RMSD graphs were generated using an in-house Python script.

Thermodynamic Calculations

The Molecular Mechanics/generalized Born surface area (MM/GBSA) is considered as the most widely used method for energetic calculations for the binding of small ligands to biological systems. [51] Although MM/GBSA method is widely used in the drug discovery process, there are still some limitations. This method is very useful for assessing relative binding affinities of studied ligands against a specific target, but it has limitations in terms of accuracy for absolute binding free energy predictions. Based on this method, enthalpy contributions provide closer calculations to

those of experimental absolute binding affinities, however entropic terms are computationally demanding and may provide large statistical uncertainties. MM/GBSA calculations were carried out using *MMPBSA.py* Python code from AmberTools17 [52,53]. The configurational entropy computed by the normal mode analysis was excluded from the analysis and only the term for formation enthalpy of the complex was considered. Neglecting entropic contributions may be critical; however, the focus here is on a ranking according to relative binding affinities (i.e., bromocriptine binding to the $D2^{High}R$ and $D2^{Low}R$) rather than absolute binding free energies. [54,55] According to the equation (1) the total binding energy is:

$$\Delta G_{bind} = G_{complex} - (G_{protein} + G_{ligand}) \qquad (1)$$

The complete details of MM/GBSA method were described in the paper by Miller et al. [52].

RESULTS AND DISCUSSION

In a post-processing analysis, the dynamics and energetics of both active ($D2^{High}R$) and inactive ($D2^{Low}R$) conformations in complex with bromocriptine were examined. Conformational and binding-mode changes of the ligand and the dynamics of the entire system, particularity in the binding pocket of the receptor, were investigated in detail. The post-processing analysis, consisting of system dynamic and thermodynamics conditions, provided information on the bromocriptine dopaminergic mechanism of interaction with the D2R binding site in both activation states.

Dynamic Profile of Bromocriptine

Conformation and transition dynamics was used to examine the degree of stability of bromocriptine binding to the receptor. The effects of bromocriptine within the active sites of the two D2R forms were monitored as a function of simulation time by calculating the RMSD values of the heavy atoms with respect to initial coordinates, as shown in **Figure 1** (The data were based on the average data of two final MD simulations). These systems were studied using two different alignment methods of trajectory frames, *ProFit* (alignment based on protein structure) and *LigFit* (alignment based on ligand atoms). Specifically, these two methods align the Cα atoms and the ligand heavy atoms, respectively. This type of strategy on alignment can provide detailed information about

translational and rotational motions of the ligand in the binding pocket. The RMSD values of the heavy atoms of ligand and the protein atoms (Cα and side chain atoms) are given as line and contour plots, respectively, in **Figure 1**. The Cα and side-chain RMSD maps are given as contour plots inside the *ProFit* and *LigFit* graphs. Structural analysis of both Cα and side chain atoms provided a much more detailed insight into the behavioral dynamics of the protein over the entire simulation for each D2R form.

Ligand Atoms: In the *ProFit* mode the mean values of the RMSDs for bromocriptine at the $D2^{High}R$ and $D2^{low}R$ were found to be 1.18 Å and 2.21 Å, respectively. Our results demonstrate that the translational motion of the ligand in the binding pocket of the $D2^{High}R$ is low relative to the motion within the binding pocket of the $D2^{Low}R$ (see trajectory video simulations S1 and S2 in the supplementary material). Thus, it can be interpreted that the chemical interactions between the ligand and the active site amino acids of the $D2^{High}R$ are effective in the structural stabilization of the ligand. These results also reflect the differential behavior of the ligand binding dynamics of both receptor conformers. On the other hand, a decrease in atomic fluctuation of the ligand in the active state reflects a decrease in entropy upon binding. Moreover, the average RMSD values of the ligand for the each simulated system ($D2^{High}R$ and $D2^{low}R$), based on the ligand atoms (*LigFit*), were determined to be 0.37 Å and 1.25 Å, respectively. These data demonstrate that the rotational motion of bromocriptine within the binding pocket of the $D2^{low}R$ was greater in comparison to the $D2^{High}R$ and was consistent with the *ProFit* data. In summary, these results suggest that bromocriptine in the binding pocket of $D2^{low}R$ forms weaker binding interactions relative to those within the $D2^{High}R$ state. Hence, bromocriptine binding within the $D2^{High}R$ state demonstrates that the lower translational and rotational motion allows for improved receptor fit as well as strong and persistent non-bonding interactions within the protein-binding site. These data were consistent with our previously reported study demonstrated that the D2R ligand-binding domain is a result of the activation process and elicits selective binding of D2R binders to the $D2^{High}R$ [10]. Thus, a relationship between the two distinct receptor conformations stabilized by the same agonist and

their signal transduction process can be derived. This change in binding selectivity of agonists or antagonists with the two D2R states may be related to slight variations in the size and shape of the binding cavity, which would allow active site amino acids to re-orient and differentially interact with the ligands.

Protein Atoms: An analysis of the dynamics of protein behavior during the simulations demonstrated that the Cα or side-chain atoms of the dimer were caused by receptor activation (**Figure 1**). The mean RMSD value of the Cα atoms for the $D2^{High}R$ and $D2^{Low}R$ were 2.71 Å and 2.52 Å, respectively, depicting very similar fluctuations. Interestingly, when the side chain atoms were considered, the side-chain atoms of the $D2^{High}R$ form fluctuated with an average RMSD value of 3.80 Å. The corresponding values for the $D2^{Low}R$ form were measured to be 3.09 Å. Side chain fluctuations for the $D2^{High}R$ and $D2^{Low}R$ were distinct, with side chain heavy atoms tending to be relatively more flexible within the $D2^{High}R$ versus the $D2^{Low}R$. The results can be interpreted as a measure of the activation state and signal propagation during conversion into a fully activated structure. Subtle structural variations of ligand within the binding pocket can profoundly impact binding affinity to the protein target. These effects can be explained by the detailed thermodynamic analyses of ligand binding, including free energy changes resulting from displacement of water molecules within the binding site. The location and thermodynamic properties of water molecules at the binding pockets of two distinct receptor conformations were slightly different. Thus, the effects of water molecules on binding and structural mobility of ligand through direct or water-bridged chemical interactions (i.e., H-bonding) may variably influence the distinct, stable receptor states. Evaluation of water molecule interactions at the start and end of simulations demonstrated that the total number of constructed chemical interactions via water molecules at simulation end were higher for the $D2^{High}R$ state. This effect may explain the more mobile character of side chains at the $D2^{High}R$.

Contour plot analyses suggest that the two D2R forms can fall into distinct pathways along the simulations. This is indicative of signal transduction across the membrane bilayers, since the conformational transition mediating signal transduction involves mutual cooperative interactions.

Additionally, the pairwise RMSD analysis of the ligand depicts the deviation of each frame from initial positions relative to other frames (**Figure 2)**. The matrix graphs give an exhaustive evaluation of the flexibility of the ligand in either the $D2^{High}R$ or $D2^{Low}R$ forms for both alignment types (that is *ProFit* and *LigFit*). The bromocriptine interactions reveal higher translational and rotational degrees of motion in the $D2^{Low}R$ state, while strong interactions between bromocriptine and $D2^{High}R$ show decreased structural motion of the ligand in $D2^{High}R$ state.

Furthermore, ligand behavior in the two forms was investigated by several feature terms, including rGyr, MolSA, SASA and PSA; these data are shown in **Figure 3**. The rGyr is a measure of ligand compactness. Based on observation, the governing system kinetics were uniform at the smaller rGyr values for the ligand in the $D2^{High}R$ state. In contrast, the corresponding values for the ligand binding to the $D2^{Low}R$ showed greater fluctuation. The rGyr results indicate that bromocriptine bound to the $D2^{High}R$ form is the more tightly packed ligand. The results were consistent with the above data from the RMSD analysis.

Moreover, the surface area of the bromocriptine ligand is monitored upon binding to either the $D2^{High}R$ or $D2^{Low}R$ states, by measuring the SASA, PSA and MolSA factors. The degree of interaction of an amino acid at the binding pocket with solvent and ligand or with other residues was proportional to the surface area exposed to these environments. The SASA result was calculated by methods involving the *in silico* rolling of a spherical probe, which models the water molecule around a protein model. The analysis depicts the relationship between the ligand surface area and the structural changes it undergoes upon binding. The surface area of the ligand that is accessible by the water molecule was introduced by SASA scanning. It was found that the D2R activation was accompanied by significant surface area transition decreases of the ligand. The PSA values, representing the surface area of the ligand contributing only by oxygen and nitrogen atoms,

were calculated as shown in **Figure 3**. A comparison of the two complexes demonstrates that the ligand in the $D2^{High}R$ has higher PSA values over the simulation. These data reveal that bromocriptine in the $D2^{Low}R$ has less potential to interact with the nitrogen and oxygen atoms of the active site amino acids due to variations in size and shape of the binding cavity. The MolSA values calculated with a probe radius of 1.4 Å were found to be largely variable for the ligand inside the $D2^{Low}R$ state suggesting that the ligand underwent diverse conformational changes in this state.

Dihedral Angle assessment: The binding of bromocriptine was also evaluated based on the change of its dihedral angle distributions throughout the simulations. This is considered to be an important feature representing the intra-dynamic profile of a molecule during MD simulations. Bromocriptine can be considered as being comprised of two structural segments: one containing the fused four ring groups linked to the 6^{th} torsional angle and the other segment connected to the 4^{th} torsional angle, as shown in **Figure 4**. The dihedral angles of bromocriptine were monitored and represented as a function of time and as histogram diagrams (**Figures 5** and **S2**). The dihedral analysis shows that the ligand mostly undergoes small conformational changes throughout the simulations in the $D2^{High}R$ state. These effects may be linked to the stronger polar and non-polar interactions formed between bromocriptine and the binding site amino acids, particularly Asp114(3.32) and Glu95(2.65). This also shows that bromocriptine is less flexible and structurally more stable in the $D2^{High}R$ state versus the $D2^{Low}R$ state. Careful investigation of each individual torsional angle of ligand shows that the 5^{th} torsional angle has mainly a *cis* conformation for $D2^{High}R$. The 6^{th} dihedral angle of bromocriptine that links the first segment of the ligand to its central region was stable in both forms, due to steric hindrance interactions surrounding the bond. Moreover, the histogram diagram representing the probability of distributions for each torsional angle during simulations is shown in **Figure S3**. The first segment is stable because of the tight ligand-receptor interactions established with both conformational states of the protein. However, the torsional angle plots and histograms of the individual dihedral angles of bromocriptine show that, although almost all defined

dihedral angles remain constant throughout simulations for $D2^{High}R$, the corresponding dihedral angles of $D2^{Low}R$ show a larger diversity, especially for the first three dihedral angles.

RMSF assessments were conducted to further examine the conformational stability or average value of fluctuations of individual amino acid during the simulations. The RMSF provided information on the average structural flexibility of the individual residues over the simulations based on the Cα (scatter plot) and side-chain (contour plot) atoms (**Figure 6)**. Based on this analysis, protomers of ligand-bound (*holo*) and ligand-free (*apo*) states were underlined. The graphs depict fluctuation increases or decreases upon ligand binding in either TM or loop segments. The 7TM domain data demonstrating greater stability relative to the loop regions, and were consistent with previously reported experimental data. It has been well established that the cytoplasmic ends of the TM5 and TM6, which are critical domains involved in G protein-coupling activation, have higher flexibility in the holo forms for both D2R states. This characteristic may describe the relationship between the presence of bromocriptine and the conformation-elicited changes on the cytoplasmic end of the TM domains. The flexibility of the cytoplasmic ends was more pronounced for the $D2^{High}R$ for the cytoplasmic segments of the TM5 and TM6 during the activation. It has been well established that full GPCR activation occurs within the millisecond timescale, and we do not claim that the movement of the cytoplasmic ends of TM5 and TM6 domains occur within the nanosecond timescale. However, the two models for the fully activated and inactivated D2R forms evaluated in this analysis was intended to provide further insights into agonist binding and the dynamics of essential amino acids for the different states. However, it should be noted that these state-of-the-art MD simulations for the active and inactive forms of D2R activation may considerably change the original system conformations, and hence the study of the receptor activation process can be perceived to be a study limit due to restricted MD time.

The amino acid Asp114 was shown to be more stable in the holo form relative to the apo state of the $D2^{High}R$ due to the strong polar interactions formed with the ligand. The C_α atoms of Phe389(6.52) were shown to be stable in the apo and holo forms of the $D2^{High}R$. This suggests that bromocriptine

binding cannot affect the Phe389(6.52), which may be due to the interactions formed by the neighboring amino acids. Moreover, the average fluctuations of the side chain atoms were calculated to have a measure of the degree of stabilization of the side chains in the $D2^{High}R$ and $D2^{low}R$ forms. In general, the side chains of the $D2^{High}R$ appeared to be more flexible relative to the $D2^{Low}R$ state, suggesting that it can be considered a measure of the activation state and signal propagation during the conversion to the fully activate structure.

Ligand-Binding Site Crevice

The per-residue decomposition analysis was carried out for the two complexes to get a better understanding of how binding space or amino acids that accommodate the ligand are impacted by the conformational transitions of the cytoplasmic ends due to the activation process. The MD trajectory frames were analyzed to identify the amino acids forming the surface of the two conformations of the D2R binding sites in complex with bromocriptine. Hydrogen bonding, hydrophobic forces, ionic bonding, π-π stacking, π-cation interactions, and water mediated interactions that formed between bromocriptine and key amino acids in the ligand-binding space were calculated **(Figure 7).** Also, the occupancy interactions of the individual amino acid residues during simulations were calculated. These data demonstrate that Asp114(3.32), His393(6.55) (backbone atoms), and Glu95(2.65) play a pivotal role in the binding space of the $D2^{High}R$, forming strong and balanced hydrogen bond interactions with the charged ligand segments. Overall, these study results were fairly consistent with the data from the Substituted Cysteine Accessibility Method (SCAM) previously reported by Javitch et al., which demonstrated that the majority of contributing amino acids were in the TM2, TM3 and TM6 segments [56-60]. In addition, Val111(3.29) and Tyr408(7.35) were previously reported to be highly pronounced and involved in hydrophobic and π-π stacking interactions, respectively [58,61]. Due to the presence of aromatic and hydrophobic residues within the binding pocket, the hydrophobic forces were regarded as a feature in accommodating the ligands inside the D2R. Other integral amino acids (present in the second extracellular loop [ECL2]) were identified as Asn176 and Cys182. The ECL2 domain,

which links the TM4 and TM5 domains, folds down into the TM domain and contributes to the ligand-binding surface [9,62]. Also, the present study suggests that Ser193(5.42) and Phe189(5.38) contributed to hydrophobic and hydrogen bonding interactions and are key residues (**Figure 7**). This is consistent with the previously reported data [63].

For $D2^{Low}R$, Ser193(5.42) was found to be a key polar residue, forming strong, stable hydrogen bonds with bromocriptine, as shown in **Figure 7**. As expected based on the nature of His393(6.55), this aromatic amino acid contributed to hydrophobic interactions with the ligand rings that are involved in π-π stacking and π-cation interactions. Interestingly, both Val111(3.29) and Asp114(3.32) appear to be moderately important residues in the active site of $D2^{low}R$, since they interact with the ligand via water-mediated bonds.

Representative 3D and 2D schematics of structures derived from the MD simulations are shown in **Figure 8.** It was evident based on these data that bromocriptine did not occupy the same topology within the binding pocket and it had variable interactions for the two D2R states. The 2D ligand interaction diagrams provide evidence around binding interactions of bromocriptine with the $D2^{High}R$ and $D2^{Low}R$ forms. The first segment of the ligand in the $D2^{High}R$ form demonstrates interactions with Glu95(2.65), Asp114(3.32), Tyr408(7.35), and His393(6.55). However, for the $D2^{Low}R$ the corresponding residues are Asp114(3.32), Ser193(5.42), and His393(6.55). It is noteworthy to highlight that Asp114(3.32) in the $D2^{High}R$ can simultaneously form two hydrogen bonds with the charged nitrogen atom and the hydroxyl group resulting in enhanced ligand stability within the cavity. These data were consistent with the conformational stability analysis, emphasizing that the ligand-binding domain of the D2R is highly altered by conformational changes that occur on the cytoplasmic ends of the TM5 and TM6 domains during the activation process [64].

Furthermore, when these data were compared to previously reported data utilizing ACR16 (D2R stabilizer), differences regarding the critical amino acids that may contribute to the binding pocket interactions of agonists and antagonists were indicated [22]. For the $D2^{High}R$ state, Asp114(3.32),

Phe389(6.52), and Phe390(6.52) were observed to be the key residues, as they formed hydrogen bonds and π-π stacking interactions with the D2R stabilizer. In contrast, the analysis of the active site of $D2^{Low}R$ in complex with a D2R stabilizer indicated that Thr112(3.30) and His393(6.55) played a pivotal role to accommodate ligand [22]. For the two complexes, with the agonist and the D2R stabilizer, Asp114(3.32) and Phe389(6.51) were integral in the binding domain of the $D2^{High}R$, whereas the agonist and the D2R stabilizer in the binding site of the $D2^{Low}R$ form revealed different key amino acids (i.e., Ser193(5.42) for the D2R agonist). Further studies must be conducted utilizing D2R activators and antagonists to make in order to arrive at conclusions regarding other agonists and antagonists of D2Rs.

Analysis of Energy of Binding

MM/GBSA calculations for the two complexes, upon bromocriptine binding to the $D2^{High}R$ and $D2^{Low}R$ states, were performed to determine changes in energy, which include van der Waals forces, electrostatic interactions, polar and non-polar solvation energies, and enthalpy binding energy, **(Table 1)**. The enthalpy terms for $D2^{High}R$ and $D2^{Low}R$ were calculated to be -58.18 kcal/mol and -47.71 kcal/mol, suggesting that bromocriptine is more selective against the $D2^{High}R$ conformation. These results were consistent with previously reported data that suggest that the K_i values of bromocriptine for the $D2^{High}R$ and $D2^{Low}R$ were 0.9 nM and 50 nM, respectively [34]. The other energy subcomponents to binding were more subtle. The MM energy values, obtained from the sum of the vdW and electrostatic terms, were found to be -68.40 kcal/mol and -67.95 kcal/mol, respectively and indicate that the formation of the two complexes and these energy values were similar. The solvation energy values, comprising polar (GB) and non-polar (NP) terms, were found to be positive and determined to be 10.22 kcal/mol and 20.23 kcal/mol for $D2^{High}R$ and $D2^{low}R$, respectively. This is due to the desolvation of polar interactions of the ligand in solution. These data were consistent and complementary to those previously obtained for the antagonist-bound systems, showing that D2R antagonists and agonists were selective for the $D2^{High}R$ form [22]. The energy data demonstrates that there is a connection between ligand-binding affinity and

conformational changes induced upon D2R activation. To date, there are only a few studies of how conformational transitions correlate with the D2R ligand interface. In summary, the energy analyses along with the other study data suggest selectivity of bromocriptine for the $D2^{High}R$ form.

CONCLUSION

In this study, the dimeric models of $D2^{High}R$ and $D2^{low}R$ in complex with bromocriptine were used to investigate in detail how the ligand-binding domain is affected by conformational changes during the activation process particularly on the cytoplasmic ends. The analysis was performed using: (i) the MM/GBSA method-based thermodynamic calculations; (ii) conformational stability analysis of the ligand and the entire system as a function of time; and (iii) investigation of the binding sites for the active ($D2^{High}R$) and inactive ($D2^{low}R$) forms of the receptor. Energy consumption assessments suggest that bromocriptine is a more selective agonist of $D2^{High}R$ ($\Delta H_{(binding)}$ = -58.18 kcal/mol) versus $D2^{Low}R$ ($\Delta H_{(binding)}$ = -47.71 kcal/mol). Also, the binding enthalpy energy data, which were consistent with previously reported data, indicated that the K_i values are 0.9 nM and 50 nM for the active and inactive forms, respectively. The analysis of dynamic features of the ligand in the two receptor conformations demonstrated a high structural stability for bromocriptine in the $D2^{High}R$ state and a higher degree of conformational flexibility within the $D2^{Low}R$ form. However, the amino acid side chains of the $D2^{High}R$ ligand-receptor complex showed more flexibility compared to the corresponding regions of the $D2^{Low}R$. Glu95, Asp114, and His393 (backbone atoms) of $D2^{High}R$ and Ser193 of $D2^{Low}R$ were found to be conserved residues for the receptor-ligand interaction. These essential amino acid residues for bromocriptine were also identified by experimental mutation analysis [56-63].

In conclusion, this in silico study focused on the ligand binding and receptor-signaling using a known D2R agonist in two distinct active and inactive receptor conformations to establish a relationship between agonist-ligand binding and the conformational transitions of the cytoplasmic ends. Focusing on a PD drug that has an elongated structure and that is accommodated well within the binding pocket of the D2R may give better insight into the behavior of elongated structural

agonists. Furthermore, this work separated out the effects of backbone and side chain atoms from the effects of conformation changes elicited upon agonist binding, thereby clarifying protein dynamics during simulations of D2R forms. In conclusion, these findings provided an initial and novel perspective regarding D2R drug binding and activation mechanisms and processes.

ASSOCIATED CONTENT

Supporting Information

Coordinate files of the $D2^{High}R$ and $D2^{Low}R$ dimer model structures (PDB)

MD trajectory frames of bromocriptine within $D2^{High}R$ (MPG)

MD trajectory frames of bromocriptine within $D2^{Low}R$ (MPG)

AUTHOR INFORMATION

Corresponding Authors

***E-mail:** ekhteiarisalmas@itu.edu.tr
***E-mail:** serdar.durdagi@med.bau.edu.tr

ORCID
Ramin Ekhteiari Salmas: 0000-0003-3888- 5070
Matthias Stein: 0000-0001-7793-0052
Serdar Durdagi: 0000-0002-0426-0905

Notes

The authors declare no competing financial interest.

ACKNOWLEDGMENTS

We thank the Max Planck Society for the Advancement of Science, the Excellence Initiative 'Center for Dynamics Systems: Systems Engineering', and the ERDF for their financial support. We acknowledge the TUBITAK ULAKBIM, High Performance and Grid Computing Center (TRUBA resources) for partially providing computational support for several analyses.

REFERENCES

1. Granier, S.; Kobilka, B. A New Era of GPCR Structural and Chemical Biology. *Nat. Chem. Biol.* **2012**, *8*, 670–673.
2. Trzaskowski, B.; Latek, D.; Yuan, S.; Ghoshdastider, U.; Debinski, A.; Filipek, S. Action of Molecular Switches in GPCRs - Theoretical and Experimental Studies. *Curr. Med. Chem.* **2012**, *19*, 1090–1109.

3. Lundstrom, K. Latest Development in Drug Discovery on G Protein-Coupled Receptors. *Curr. Protein Pept. Sci.* **2006**, *7*, 465–470.
4. Stevens, R. C.; Cherezov, V.; Katritch, V.; Abagyan, R.; Kuhn, P.; Rosen, H.; Wüthrich, K. The GPCR Network: A Large-Scale Collaboration to Determine Human GPCR Structure and Function. *Nature Reviews Drug Discovery*. **2013**, *12*, 25–34.
5. Kobilka, B. K. G Protein Coupled Receptor Structure and Activation. *Biochim. Biophys. Acta - Biomembr.* **2007**, *1768*, 794–807.
6. Shonberg, J.; Kling, R. C.; Gmeiner, P.; Löber, S. GPCR Crystal Structures: Medicinal Chemistry in the Pocket. *Bioorganic Med. Chem.* **2015**, *23*, 3880–3906.
7. Simms, J.; Hall, N. E.; Lam, P. H. C.; Miller, L. J.; Christopoulos, A.; Abagyan, R.; Sexton, P. M. Homology Modeling of GPCRs. *Methods Mol. Biol.* **2009**, *552*, 97–113.
8. Ballesteros, J.; Palczewski, K. G Protein-Coupled Receptor Drug Discovery: Implications from the Crystal Structure of Rhodopsin. *Curr. Opin. Drug Discov. Devel.* **2001**, *4*, 561–574.
9. Salmas, R. E.; Yurtsever, M.; Stein, M.; Durdagi, S. Modeling and Protein Engineering Studies of Active and Inactive States of Human Dopamine D2 Receptor (D2R) and Investigation of Drug/receptor Interactions. *Mol. Divers.* **2015**, *19*, 321–332.
10. Durdagi, S.; Salmas, R. E.; Stein, M.; Yurtsever, M.; Seeman, P. Binding Interactions of Dopamine and Apomorphine in D2High and D2Low States of Human Dopamine D2 Receptor Using Computational and Experimental Techniques. *ACS Chem. Neurosci.* **2016**, *7*, 185–195.
11. Rosenbaum, D. M.; Rasmussen, S. G. F.; Kobilka, B. K. The Structure and Function of G-Protein-Coupled Receptors. *Nature* **2009**, *459*, 356–363.
12. Simms, J.; Hall, N. E.; Lam, P. H. C.; Miller, L. J.; Christopoulos, A.; Abagyan, R.; Sexton, P. M. Homology Modeling of GPCRs. *Methods Mol. Biol.* **2009**, *552*, 97–113.
13. Worth, C. L.; Kleinau, G.; Krause, G. Comparative Sequence and Structural Analyses of G-Protein-Coupled Receptor Crystal Structures and Implications for Molecular Models. *PLoS One* **2009**, *4*, e701.
14. Venkatakrishnan, A. J.; Deupi, X.; Lebon, G.; Tate, C. G.; Schertler, G. F.; Babu, M. M. Molecular Signatures of G-Protein-Coupled Receptors. *Nature* **2013**, *494*, 185–194.
15. Seeman; Chau-Wong, M.; Tedesco, J.; Wong, K. Brain Receptors for Antipsychotic Drugs and Dopamine: Direct Binding Assays. *Proc. Natl. Acad. Sci. U. S. A.* **1975**, *72*, 4376–4380.
16. Madras, B. K. History of the Discovery of the Antipsychotic Dopamine D2 Receptor: A Basis for the Dopamine Hypothesis of Schizophrenia. *J. Hist. Neurosci.* **2013**, *22*, 62–78.
17. Usiello, a; Baik, J. H.; Rougé-Pont, F.; Picetti, R.; Dierich, a; LeMeur, M.; Piazza, P. V; Borrelli, E. Distinct Functions of the Two Isoforms of Dopamine D2 Receptors. *Nature* **2000**, *408*, 199–203.
18. Gerfen, C. R. Indirect-Pathway Neurons Lose Their Spines in Parkinson Disease. *Nature Neuroscience*. ***2006***, *9*, 157–158.
19. Baik, J.-H.; Picetti, R.; Saiardi, A.; Thiriet, G.; Dierich, A.; Depaulis, A.; Le Meur, M.; Borrelli, E. Parkinsonian-like Locomotor Impairment in Mice Lacking Dopamine D2 Receptors. *Nature* **1995**, 377, 424–428.
20. Seeman, P. Targeting the Dopamine D2 Receptor in Schizophrenia. *Expert Opin. Ther. Targets* **2006**, *10*, 515–531.
21. Seeman, P. Dopamine D2 Receptors as Treatment Targets in Schizophrenia. *Clin. Schizophr. Relat. Psychoses* **2010**, *4*, 56–73.

22. Ekhteiari Salmas, R.; Seeman, P.; Aksoydan, B.; Stein, M.; Yurtsever, M.; Durdagi, S. Biological Insights of the Dopaminergic Stabilizer ACR16 at the Binding Pocket of Dopamine D2 Receptor. *ACS Chem. Neurosci.* **2017**, *8*, 826–836.
23. Khelashvili, G.; Dorff, K.; Shan, J.; Camacho-Artacho, M.; Skrabanek, L.; Vroling, B.; Bouvier, M.; Devi, L. a; George, S. R.; Javitch, J. a; Lohse, M. J.; Milligan, G.; Neubig, R. R.; Palczewski, K.; Parmentier, M.; Pin, J.-P.; Vriend, G.; Campagne, F.; Filizola, M. GPCR-OKB: The G Protein Coupled Receptor Oligomer Knowledge Base. *Bioinformatics* **2010**, *26*, 1804–1805.
24. Teitler, M.; Klein, M. T. A New Approach for Studying GPCR Dimers: Drug-Induced Inactivation and Reactivation to Reveal GPCR Dimer Function in Vitro, in Primary Culture, and in Vivo. *Pharmacology and Therapeutics*. **2012**, *133*, 205–217.
25. Li, G.; Haney, K. M.; Kellogg, G. E.; Zhang, Y. Comparative Docking Study of Anibamine as the First Natural Product CCR5 Antagonist in CCR5 Homology Models. *J. Chem. Inf. Model.* **2009**, *49*, 120–132.
26. Verma, V.; Hasbi, A.; O'Dowd B.F.; George, S. R. Dopamine D1-D2 Receptor Heteromer-Mediated Calcium Release Is Desensitized by D1 Receptor Occupancy with or without Signal Activation: Dual Functional Regulation by G Protein-Coupled Receptor Kinase 2. *J. Biol. Chem.* **2010**, *285*, 35092–35103.
27. Guo, W.; Shi, L.; Javitch, J. A. The Fourth Transmembrane Segment Forms the Interface of the Dopamine D2 Receptor Homodimer. *J. Biol. Chem.* **2003**, *278* (7), 4385–4388.
28. Armstrong, D.; Strange, P. G. Dopamine D2 Receptor Dimer Formation: Evidence from Ligand Binding. *J Biol Chem* **2001**, *276*, 22621–22629.
29. Lee, S. P.; O'Dowd, B. F.; Rajaram, R. D.; Nguyen, T.; George, S. R. D2 Dopamine Receptor Homodimerization Is Mediated by Multiple Sites of Interaction, Including an Intermolecular Interaction Involving Transmembrane Domain 4. *Biochemistry* **2003**, *42*, 11023–11031.
30. Fotiadis, D.; Liang, Y.; Filipek, S.; Saperstein, D. A.; Engel, A.; Palczewski, K. Rhodopsin Dimers in Native Disc Membranes. *Nature* **2003**, *421*, 127–128.
31. Petersen, J.; Wright, S. C.; Rodríguez, D.; Matricon, P.; Lahav, N.; Vromen, A.; Friedler, A.; Strömqvist, J.; Wennmalm, S.; Carlsson, J.; Schulte, G. Agonist-Induced Dimer Dissociation as a Macromolecular Step in G Protein-Coupled Receptor Signaling. *Nat. Commun.* **2017**, *8*, 226.
32. Guo, W.; Shi, L.; Filizola, M.; Weinstein, H.; Javitch, J. A. From The Cover: Crosstalk in G Protein-Coupled Receptors: Changes at the Transmembrane Homodimer Interface Determine Activation. *Proc. Natl. Acad. Sci.* **2005**, *102*, 17495–17500.
33. Periole, X.; Knepp, A. M.; Sakmar, T. P.; Marrink, S. J.; Huber, T. Structural Determinants of the Supramolecular Organization of G Protein-Coupled Receptors in Bilayers. *J. Am. Chem. Soc.* **2012**, *134*, 10959–10965.
34. Seeman, P. Antiparkinson Therapeutic Potencies Correlate with Their Affinities at Dopamine D2High Receptors. *Synapse* **2007**, *61*, 1013–1018.
35. Lieberman, A. N.; Goldstein, M. Bromocriptine in Parkinson Disease. *Pharmacol. Rev.* **1985**, *37*, 217–227.
36. Seeman, P. Parkinson's Disease Treatment May Cause Impulse-Control Disorder via Dopamine D3 Receptors. *Synapse* **2015**, *69*, 183–189.
37. Schrödinger Release 2015-2: LigPrep, Schrödinger, LLC, New York, NY, 2017.

38. Shelley, J. C.; Cholleti, A.; Frye, L. L.; Greenwood, J. R.; Timlin, M. R.; Uchimaya, M. Epik: A Software Program for pKa Prediction and Protonation State Generation for Drug-like Molecules. *J. Comput. Aided. Mol. Des.* **2007**, *21*, 681–691.
39. Banks, J. L.; Beard, H. S.; Cao, Y.; Cho, A. E.; Damm, W.; Farid, R.; Felts, A. K.; Halgren, T. A.; Mainz, D. T.; Maple, J. R.; Murphy, R.; Philipp, D. M.; Repasky, M. P.; Zhang, L. Y.; Berne, B. J.; Friesner, R. A.; Gallicchio, E.; Levy, R. M. Integrated Modeling Program, Applied Chemical Theory (IMPACT). *Journal of Computational Chemistry*. **2005**, *26*, 1752–1780.
40. Dewar, M. J. S.; Zoebisch, E. G.; Healy, E. F.; Stewart, J. J. P. Development and Use of Quantum Mechanical Molecular Models. 76. AM1: A New General Purpose Quantum Mechanical Molecular Model. *J. Am. Chem. Soc.* **1985**, *107*, 3902–3909.
41. Chien, E. Y. T.; Liu, W.; Zhao, Q.; Katritch, V.; Han, G. W.; Hanson, M. A.; Shi, L.; Newman, A. H.; Javitch, J. A.; Cherezov, V.; Stevens, R. C. Structure of the Human Dopamine D3 Receptor in Complex with a D2/D3 Selective Antagonist. *Science* **2010**, *330*, 1091–1095.
42. Bas, D. C.; Rogers, D. M.; Jensen, J. H. Very Fast Prediction and Rationalization of pKa Values for Protein-Ligand Complexes. *Proteins Struct. Funct. Genet.* **2008**, *73*, 765–783.
43. Sherman, W.; Day, T.; Jacobson, M. P.; Friesner, R. A.; Farid, R. Novel Procedure for Modeling Ligand/receptor Induced Fit Effects. *J. Med. Chem.* **2006**, *49*, 534–553.
44. Mark, P.; Nilsson, L. Structure and Dynamics of the TIP3P, SPC, and SPC/E Water Models at 298 K. *J. Phys. Chem. A* **2001**, *105*, 9954–9960.
45. Desmond Bowers, K., Chow, E., Xu, H., Dror, R., Eastwood, M., Gregersen, B., Klepeis, J., Kolossvary, I., Moraes, M., Sacerdoti, F., Salmon, J., Shan, Y., and Shaw, D. (2006) Scalable Algorithms for Molecular Dynamics Simulations on Commodity Clusters. ACM/ IEEE Conference on Supercomputing (SC06), Tampa, FL, November, **2006,** 11−17.
46. Essmann, U.; Perera, L.; Berkowitz, M. L.; Darden, T.; Lee, H.; Pedersen, L. G. A Smooth Particle Mesh Ewald Method. *J. Chem. Phys.* **1995**, *103*, 8577–8593.
47. Hoover, W. G. Canonical Dynamics: Equilibrium Phase-Space Distributions. *Phys. Rev. A* **1985**, *31*, 1695–1697.
48. Martyna, G. J.; Tobias, D. J.; Klein, M. L. Constant Pressure Molecular Dynamics Algorithms. *J. Chem. Phys.* **1994**, *101*, 4177–4189.
49. Hunter, J. D. Matplotlib: A 2D Graphics Environment. *Comput. Sci. Eng.* **2007**, *9*, 99–104.
50. Van Der Walt, S.; Colbert, S. C.; Varoquaux, G. The NumPy Array: A Structure for Efficient Numerical Computation. *Comput. Sci. Eng.* **2011**, *13*, 22–30.
51. Genheden, S.; Ryde, U. Comparison of the Efficiency of the LIE and MM/GBSA Methods to Calculate Ligand-Binding Energies. *J. Chem. Theory Comput.* **2011**, *7*, 3768–3778.
52. Miller, B. R.; McGee, T. D.; Swails, J. M.; Homeyer, N.; Gohlke, H.; Roitberg, A. E. MMPBSA.py: An Efficient Program for End-State Free Energy Calculations. *J. Chem. Theory Comput.* **2012**, *8*, 3314–3321.
53. Case, D. A.; Betz, R. M.; Botello-Smith, W.; Cerutti, D. S.; Cheatham, T. E.; III, Darden, T. A.; Duke, R. E.; Giese, T. J.; Gohlke, H.; Goetz, A. W., Homeyer, N., Izadi, S., Janowski, P., Kaus, J.; Kovalenko, A.; Lee, T. S.; LeGrand, S.; Li, P.; Lin, C.; Luchko, T.; Luo, R.; Madej, B.; Mermelstein, D.; Merz, K. M.; Monard, G.; Nguyen, H.; Nguyen, H. T.; Omelyan, I.; Onufriev, A.; Roe, D. R.; Roitberg, A.; Sagui, C.; Simmerling, C. L.; Swails, J.; Walker, R. C.; Wang, J.; Wolf, R. M.; Wu, X.; Xiao, L.; York, D. M.; and Kollman, P. A. AMBER 2016; University of California, San Francisco; 2016.

54. Yang, T.; Wu, J. C.; Yan, C.; Wang, Y.; Luo, R.; Gonzales, M. B.; Dalby, K. N.; Ren, P. Virtual Screening Using Molecular Simulations. *Proteins Struct. Funct. Bioinforma.* **2011**, *79*, 1940–1951.
55. Wang, C.; Greene, D.; Xiao, L.; Qi, R.; Luo, R. Recent Developments and Applications of the MMPBSA Method. *Front. Mol. Biosci.* **2018**, *4*, 1–18.
56. Javitch, J. A.; Ballesteros, J. A.; Weinstein, H.; Chen, J. A Cluster of Aromatic Residues in the Sixth Membrane-Spanning Segment of the Dopamine D2 Receptor Is Accessible in the Binding-Site Crevice. *Biochemistry* **1998**, *37*, 998–1006.
57. Javitch, J. A.; Ballesteros, J. A.; Chen, J.; Chiappa, V.; Simpson, M. M. Electrostatic and Aromatic Microdomains within the Binding-Site Crevice of the D2 Receptor: Contributions of the Second Membrane-Spanning Segment. *Biochemistry* **1999**, *38*, 7961–7968.
58. Javitch, J. A.; Fu, D.; Chen, J.; Karlin, A. Mapping the Binding-Site Crevice of the Dopamine D2 Receptor by the Substituted-Cysteine Accessibility Method. *Neuron* **1995**, *14*, 825–831.
59. Jonathan, A.; Li, X.; Kaback, J. A cysteine residue in the third membrane-spanning segment of the human D2 dopamine receptor is exposed in the binding-site crevice. *Proc. Natl. Acad. Sci. U. S. A* **1994**, *91*,10355-10359
60. Javitch, J. A.; Ballesteros, J. A.; Weinstein, H.; Chen, J. A Cluster of Aromatic Residues in the Sixth Membrane-Spanning Segment of the Dopamine D2 Receptor Is Accessible in the Binding-Site Crevice. *Biochemistry* **1998**, *37*, 998–1006.
61. Fu, D.; Ballesteros, J. a; Weinstein, H.; Chen, J.; Javitch, J. a. Residues in the Seventh Membrane-Spanning Segment of the Dopamine D2 Receptor Accessible in the Binding-Site Crevice. *Biochemistry* **1996**, *35*, 11278–11285.
62. Shi, L.; Javitch, J. a. The Second Extracellular Loop of the Dopamine D2 Receptor Lines the Binding-Site Crevice. *Proc. Natl. Acad. Sci. U. S. A.* **2004**, *101*, 440–445.
63. Javitch, J. A. Residues in the fifth membrane-spanning segment of the dopamine D2 receptor exposed in the binding-site crevice. *Biochemistry* **1995**, *34*, 16433-16439.
64. Rasmussen, S. G.; DeVree, B. T.; Zou, Y.; Kruse, A. C.; Chung, K. Y.; Kobilka, T. S.; Thian, F. S.; Chae, P. S.; Pardon, E.; Calinski, D.; Mathiesen, J. M.; Shah, S. T.; Lyons, J. A.; Caffrey, M.; Gellman, S. H.; Steyaert, J.; Skiniotis, G.; Weis, W. I.; Sunahara, R. K.; Kobilka, B. K. Crystal Structure of the β2 Adrenergic Receptor-Gs Protein Complex. *Nature* **2011**, *477*, 549–555.

TABLES

Table 1. Energetic analysis of bromocriptine in complex with the homodimeric $D2^{High}R$ and $D2^{Low}R$, as obtained by the MM-GBSA method.

Energy term	Mean value (kcal/mol) ± SEM[a]	
	$D2^{high}R$–$D2^{high}R$	$D2^{low}R$–$D2^{low}R$
ΔE_{vdw}	-75.83 ± 0.34	-59.87 ± 0.43
ΔE_{elec}	7.42 ± 1.10	-8.07 ± 0.89
ΔE_{MM}	-68.40 ± 1.18	-67.95 ± 1.05
ΔG_{GB}	19.47 ± 0.92	27.15 ± 0.84
ΔG_{NP}	-9.25 ± 0.02	-6.92 ± 0.05
ΔG_{solv}	10.22 ± 0.92	20.23 ± 0.83
$\Delta G_{elec(tot)}$	26.90 ± 1.01	19.08 ± 0.86
$\Delta H_{(binding)}$	-58.18 ± 0.50	-47.71 ± 0.48
$K_{i\ (Exp.)}$ [34]	0.9 (nM)	50 (nM)

[a]Standard error of the mean (SEM)

FIGURES

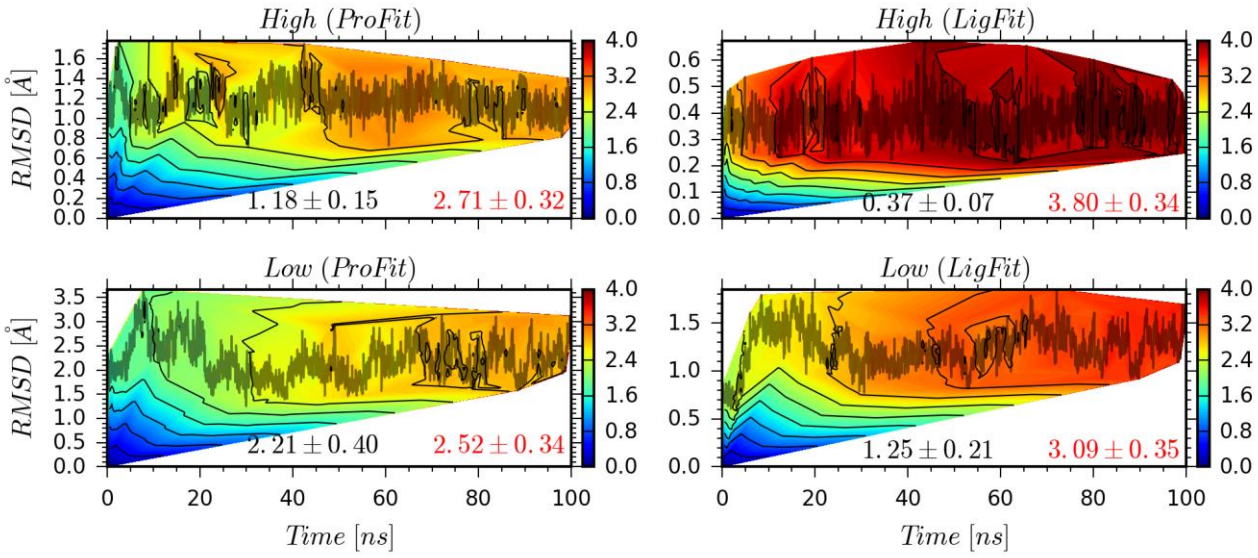

Figure 1. RMSDs of the heavy atoms of the ligand (line plots) and Cα (two left contour plots) as well as side chain atoms of proteins (two right contour plots) relative to their initial positions monitored during the MD simulations. The data were obtained from average of two final MD simulations. The RMSD mean values were calculated for the ligand and protein atoms (included at the graphs with black and red colors, respectively). The *ProFit* and *LigFig* plots show the types of alignment for trajectories, describing when the frames that were aligned based on the Cα and ligand atoms, respectively. The Cα and side-chain RMSD maps were respectively profiled as contour plots inside the *ProFit* and *LigFit* graphs. The mean RMSD values were calculated for the ligand (black) and protein (red).

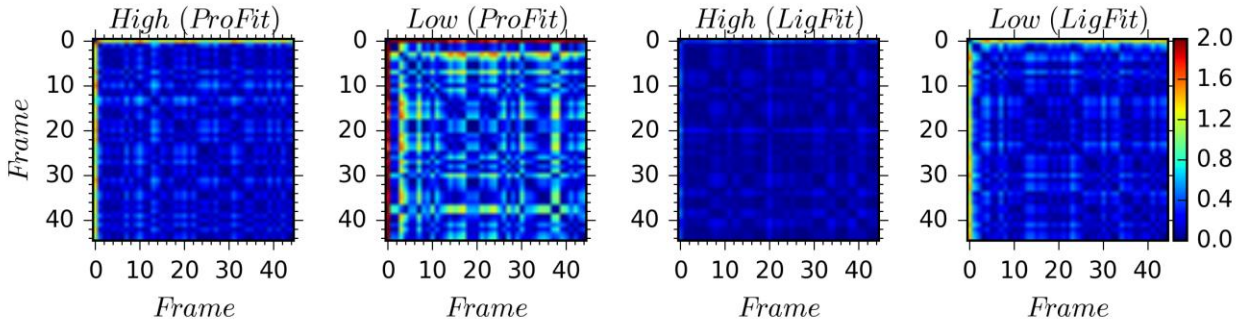

Figure 2. Pairwise RMSD analysis of bromocriptine in the active and inactive forms. Two different alignment styles were used. The matrices were designed to present the RMSD of each frame relative to the other frames.

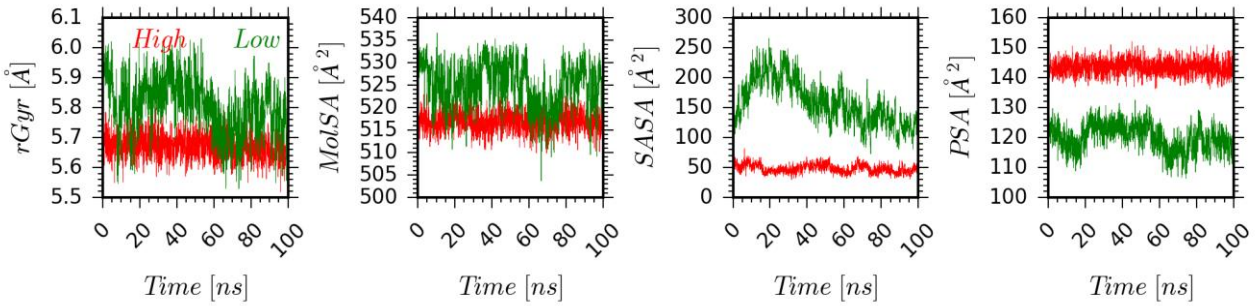

Figure 3. RGyr, MolSA, SASA, and PSA parameters were calculated for bromocriptine in the binding domains of the active and inactive D2R conformations throughout each simulation.

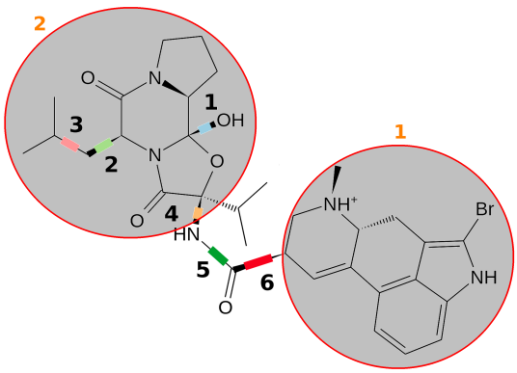

Figure 4. The chemical structure of bromocriptine, showing the six-dihedral angles with different colors.

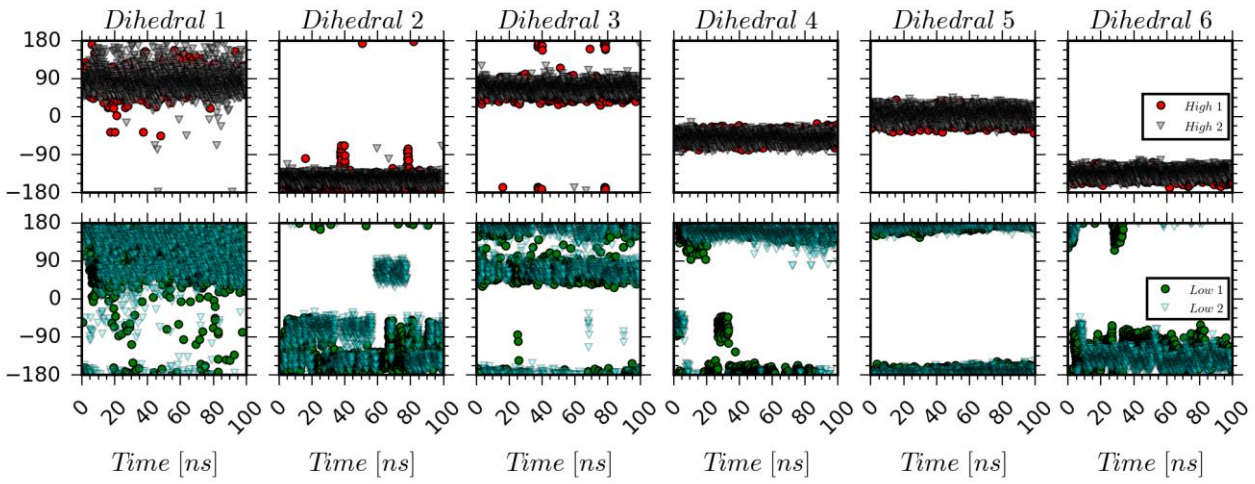

Figure 5. Dihedral angle changes of bromocriptine in $D2^{High}R$ (active state; upper panel) and $D2^{Low}R$ (inactive state; lower panel) monitored as a function of simulation time.

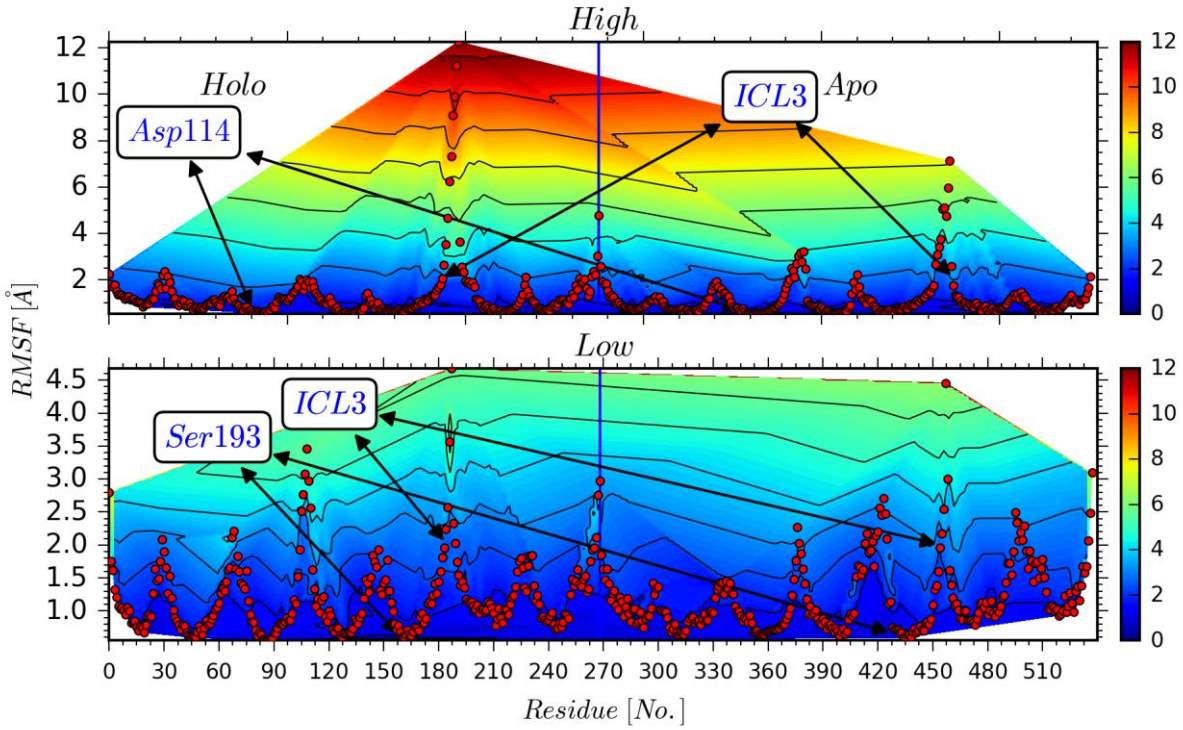

Figure 6. RMSF (Å) values for individual amino acids based on Cα (scatter plot) and side chain atoms (contour plot). The highlighted amino acids depicted in the profile play a an integral role in ligand stabilization.

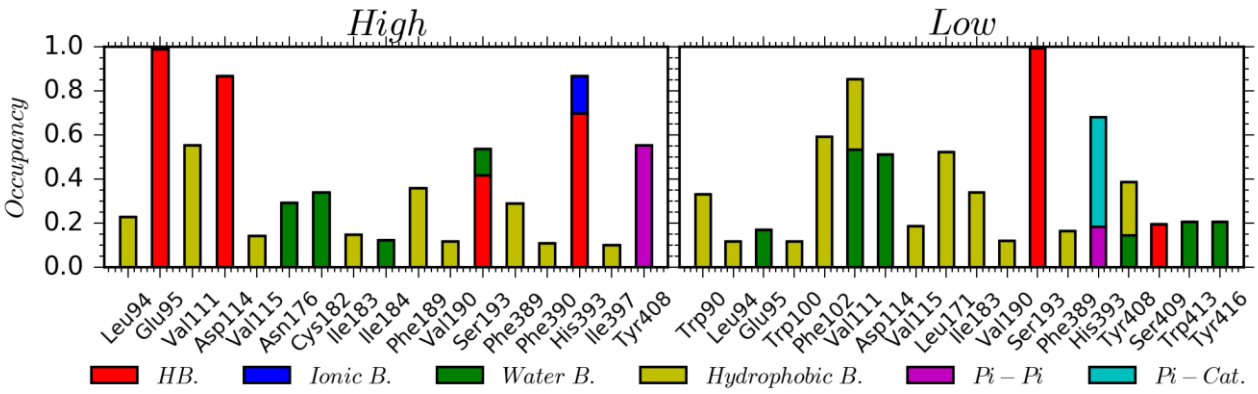

Figure 7. Interactions of the active site amino acids, hydrogen bonds (HB), water bridges (WB), and hydrophobic (HPH) interactions are profiled. Fraction 1 for an interaction means that this interaction was conserved all over the simulation (100% occupancy). The major residues formed stable interaction with the ligand were determined to be Asp114(3.32) and Glu95(2.65) for the active form and Ser193(5.42) for the inactive state of the D2R.

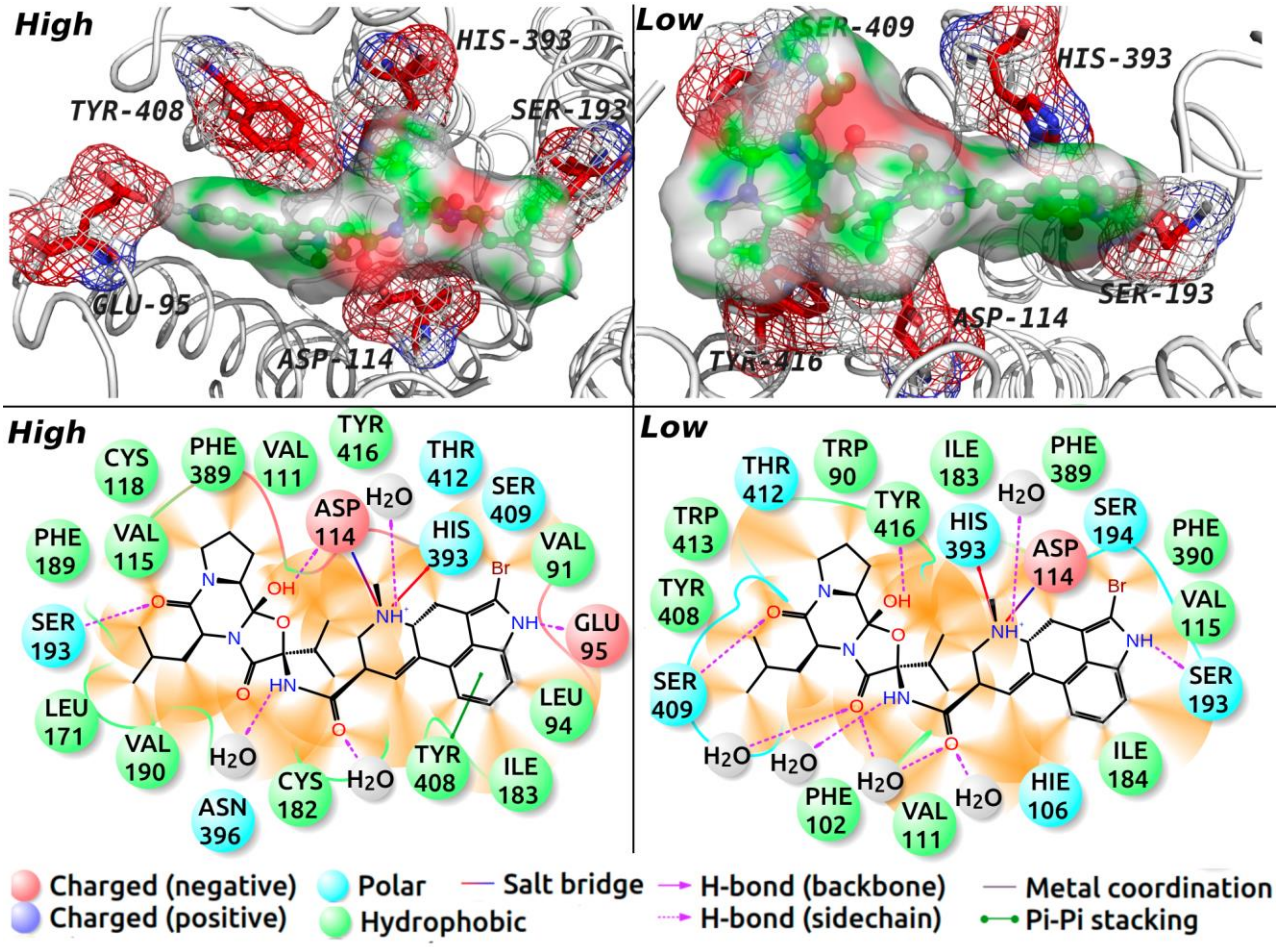

Figure 8. (top) Representative 3D schematic views of the binding domains of $D2^{High}R$ (left) and $D2^{Low}R$ (right), obtained from MD trajectory frames. Bromocriptine binding configurations, electron density, and active site amino acids considered to be pivotal in ligand stabilization are shown. **(bottom)** Representative 2D schematic views from MD simulations of bromocriptine configurations active site amino acid interactions for the $D2^{High}R$ and $D2^{Low}R$ states. The amino acids within 4 Å of the ligand are shown. The properties of the amino acids and the major interactions formed inside the cavity are represented by distinct colors and symbols. Asp114(3.32) and Glu95(2.65) are considered the critical residues involved in the stabilization of the first segment of bromocriptine within the binding pocket of the active state.